Phase-Matching Properties of $BaGa_4S_7$ and $BaGa_4Se_7$: Wide-Bandgap Nonlinear Crystals for the Mid-Infrared

Valeriy Badikov, Dmitrii Badikov, Galina Shevyrdyaeva
High Technologies Laboratory, Kuban State University, 149 Stavropolskaya Str., 350040 Krasnodar, Russia

Aleksey Tyazhev, Georgi Marchev, Vladimir Panyutin, Valentin Petrov
Max-Born-Institute for Nonlinear Optics and Ultrafast Spectroscopy, 2A Max-Born-Str., D-12489 Berlin, Germany
petrov@mbi-berlin.de

Albert Kwasniewski
Leibniz Institute for Crystal Growth, 2 Max-Born-Str., D-12489 Berlin, Germany

Abstract: Biaxial $BaGa_4S_7$ and $BaGa_4Se_7$ crystals have been grown by the Bridgman-Stockbarger technique in sufficiently large sizes and with good optical quality to measure the refractive indices and analyze the phase-matching configurations.

OCIS codes: (160.4330) Nonlinear optical materials; (190.4410) Nonlinear optics, parametric processes.

1. Introduction

At present, there is increasing interest in non-oxide nonlinear crystals that can be used for transformation of high-power solid-state lasers systems operating near 1 μm (e.g. Nd:YAG at 1064 nm) to the mid-IR above ~5 μm, the upper wavelength cut-off limit of oxide materials. In order to avoid two-photon absorption, the bandgap of such crystals should correspond to a wavelength <532 nm, a condition which is satisfied by only few chalcogenide compounds. The most prominent of them is the commercially available chalcopyrite type $AgGaS_2$ (AGS). Other crystals with relatively wide bandgap include the related defect chalcopyrite $HgGa_2S_4$, which is extremely difficult to grow, the orthorhombic $LiGaS_2$, $LiInS_2$, $LiGaSe_2$ and $LiInSe_2$ compounds which exhibit relatively low nonlinearities, the recently developed chalcopyrite $CdSiP_2$, which exhibits exceptionally high nonlinearity and can be non-critically phase-matched but unfortunately transmits only up to ~6.5 μm, as well as some solid solutions whose composition is almost impossible to control in the growth process [1]. Two new compounds can be now added to this short list, $BaGa_4S_7$ (BGS) and $BaGa_4Se_7$ (BGSe), and as it will be shown here, both of them exhibit phase-matching capability to cover the mid-IR spectral range by down-conversion of 1064 nm laser radiation.

2. Crystal growth

The non-centrosymmetric orthorhombic structure of BGS was identified as early as 1983 [2]. Recently, single crystals of BGS were grown by the Bridgman-Stockbarger technique and the SHG effect was confirmed by the Kurtz powder test [3]. While the bandgap was estimated in [3] to correspond to ~350 nm (3.54 eV) and the transparency to extend up to 13.7 μm at the 0-level, no information exists on the dispersive properties of BGS.

We successfully grew BGS and for the first time its selenide analogue, BGSe, by the Bridgman-Stockbarger method in sizes sufficiently large to measure the dispersion of the refractive indexes, a prerequisite for the prediction of the phase-matching properties. The raw materials used to synthesize the charge were with high purity, 6Ns for Ga, S and Se, and 99% for Ba. Because of the pronounced chemical activity of Ba, the synthesis took place in glass-carbon containers, evacuated to a residual pressure of 2×10^{-5} torr.

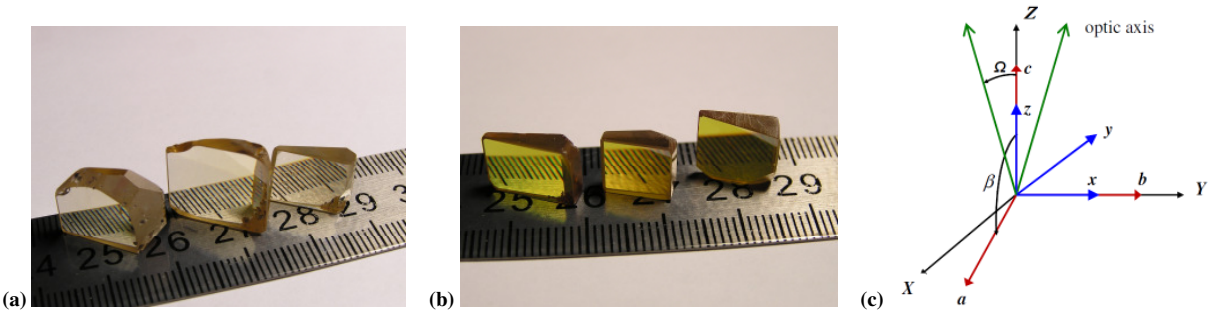

Fig. 1. Prisms of (a) BGS and (b) BGSe prepared for refractive index measurements. (c) Crystallographic (*abc*), crystallo-physical (*XYZ*) and dielectric (*xyz*) frames of BGSe. All frames are right-handed. The *b*-axis is normal to the *a*-*c* plane and the *a*-*c* plane contains the *y*≡-*X* axes. The two optic axes (green arrows) lie in the *x*-*z* plane.

The temperature in the synthesis furnace was initially raised to 1150°C at 200°C/h and the charge was held at this temperature for a few hours in order to homogenize it, after that the oven was switched-off to cool the charge down to room temperature. Then the charge was loaded into quartz ampoules of ϕ18×150 mm size which were evacuated again to residual pressure of 2×10^{-5} torr and inserted into the heating zone of the growth furnace. The temperature was raised to 1130-1140°C (BGS) and 1070-1080°C (BGSe) and after 3 h the ampoule was lowered into the crystallization zone. In order to avoid the contact between the melt and the quartz, the inner wall of the ampoule was with carbon fettling. We estimated melting temperature of 1105±5°C for BGS and 1050±5°C for BGSe. The optimum parameters for the crystal growth were derived from several preliminary experiments by assessing the optical quality of the grown crystals. The optimum crystallization rate is in the 7±2 mm/day range, the temperature gradient in the crystallization zone is 15±2 °C/cm and the characteristic growth time is 12-15 days.

The as-grown crystals are colorless in the case of BGS (Fig. 1a) and light-yellow in the case of BGSe (Fig. 1b). The good transmission limits for such initial samples, estimated at an absorption level of 0.3 cm^{-1} from unpolarized transmission spectra, are 0.545-9.4 µm (BGS) and 0.776-14.72 µm (BGSe). As for BGS [3], the short wave limit of BGSe seems also quite shifted to the red with respect to the bandgap which we estimated to be at 469 nm (2.64 eV) at the 0-level transmission. Thus in both crystals no two-phonon absorption should be expected at 1064 nm.

3. Optical ellipsoid and refractive indices

Both crystals are biaxial but while BGS is orthorhombic (*mm*2 point group), BGSe is monoclinic (*m*-point group). We determined the orientation of the dielectric frames (optical ellipsoids) from conoscopic pictures using 633 nm laser light. The three principal dielectric axes and the two optic axes were identified. For both compounds, three prisms were prepared for measurements of the index of refraction using the auto-collimation method with the reflecting face always coinciding with one of the principal planes. The accuracy in the orientation of this face was better than 0.5°, the aperture was larger than 10×12 mm^2 and the refraction angles were in the 10-14° range. Using three instead of two prisms allowed us to estimate the error in the index measurements which was <0.003 in the 1-2 µm wavelength range. The principal refractive index measurements were performed in the 0.42-9.5 µm spectral range for BGS and between 0.48 and 10.4 µm for BGSe. Two-pole Sellmeier equations were then fitted to the experimental data. These equations reproduced rather well the angle Ω between the optic axes (see the green arrows in Fig. 1c) and the z-principal (dielectric) axis (under the convention $n_x<n_y<n_z$): Ω=46.3° (BGS) and Ω=25.5° (BGSe) while the experimental values were Ω=45.6° (BGS) and Ω=26.3° (BGSe). Thus, BGSe is an optically positive biaxial crystal while BGS is one of the rare examples of equidistant refractive indices in a biaxial crystal which means greater variety of phase-matched interactions in the *x*-*z* principal plane. The computed refractive indices at 1064.2 nm amount to n_x=2.28153, n_y=2.30104 and n_z=2.32175 for BGS, and n_x=2.48615, n_y=2.50245 and n_z=2.55872 for BGSe. Hence, the maximum birefringence at this wavelength (~0.04 for BGS and ~0.07 for BGSe) is obviously sufficient for phase-matching.

In order to determine in which principal planes phase-matched processes exhibit non-vanishing effective nonlinearity d_{eff}, it is imperative to identify the two-fold axis of BGS and the correspondence between the dielectric (*xyz*) and crystallographic (*abc*) axes in both crystals. The two-fold axis of BGS was determined to coincide with the *c*-crystallographic axis from non-phase-matched SHG generation using amplified femtosecond pulses at 1300 nm and propagation along the three principal axes. The correspondence in the orthorhombic BGS crystal is *xyz*=*cab* if the convention $c_0<a_0<b_0$ is used for the lattice parameters. In monoclinic crystals one of the principal axes always coincides with the *b*-crystallographic axis and from X-ray measurements we established that for BGSe this is the *x*-principal axis. At 633 nm, the *y*-principal axis of BGSe, within ±0.5° uncertainty, is antiparallel to the *X*-crystallo-physical axis, and the *z*-principal axis coincides with the *c*-crystallographic or *Z* crystallo-physical axis (assuming $c_0<a_0$ as standard for monoclinic crystals). Note that the crystallo-physical frame *XYZ* is an orthogonal frame for reporting tensor properties with two axes coinciding per definition with the crystallographic *b*- and *c*-axes (see Fig. 1c). It is interesting that for the BGSe crystal the tensor elements of the second-order nonlinear susceptibility, d_{il} can be defined and measured directly in the *xyz* frame since it coincides with the crystallo-physical frame *XYZ*.

4. Phase-matching properties

The calculated second-harmonic generation (SHG) phase-matching curves for BGS, fundamental wavelength versus phase-matching angle, are shown in Fig. 2 for the three principal planes. Only types of interaction are included that exhibit non-vanishing d_{eff}. For SHG these are only type-I interactions, negative (oo-e) in the *x*-*y* and *x*-*z* planes and positive type (ee-o) in the *y*-*z* principal plane.

With respect to down conversion of high-power radiation from 1064 nm to the mid-IR using three-wave interactions, BGS is phase-matchable in the *x*-*y* plane (oo-e) for idler wavelengths only up to 5.42 µm where d_{eff} vanishes. In the *y*-*z* plane, phase-matching (ee-o) is possible up to 6.23 µm at which wavelength the non-critical

configuration is combined with non-zero nonlinearity. Most promising seems oo-e interaction in the *x*-*z* plane, where phase-matching is possible at idler wavelengths starting from 6.23 µm in the non-critical configuration and with maximum d_{eff} up to the mid-IR transmission cut-off of BGS. Wavelengths near 6.45 µm, interesting for medical applications, could be possibly achieved by temperature tuning in the non-critical configuration. In this plane also type-II (oe-o) interaction is possible but it starts from idler wavelengths of 8.05 µm where d_{eff} is vanishing and this nonlinearity remains small within the entire possible idler tuning range.

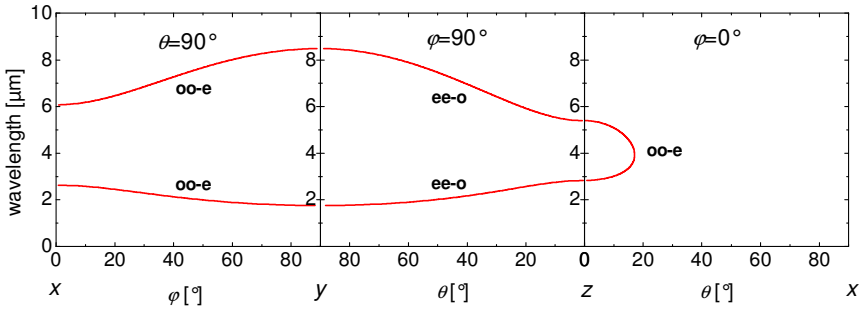

Fig. 2. Phase-matching for SHG in the three principal planes of BGS for interactions with non-vanishing effective nonlinearity.

The calculated SHG phase-matching curves for BGSe are shown in Fig. 3 for the three principal planes. As can be seen, more polarization configurations exist due to the lower symmetry and only type-I interaction (ee-o) in the *y*-*z* plane is with vanishing d_{eff}. Thus SHG is possible in the entire transparency range of BGSe with few non-critical configurations along the three principal dielectric axes. All non-critical configurations for propagation along the *x*-axis exhibit non-vanishing d_{eff} while for propagation along the *y*-axis this is only type-II interaction. Among the fundamental wavelengths that could be possibly non-critically phase-matched by temperature tuning is also the CO_2 laser wavelength at 10.6 µm.

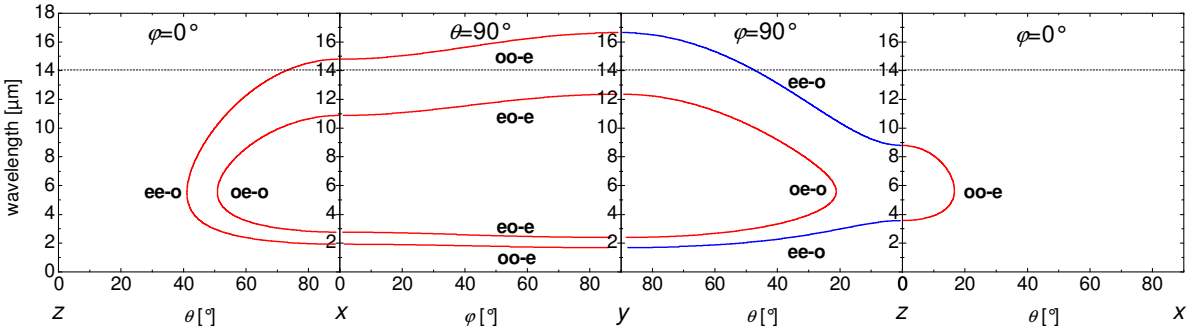

Fig. 3. Phase-matching for SHG in the three principal planes of BGSe for interactions with non-vanishing effective nonlinearity (red lines) and vanishing effective nonlinearity (blue lines). The dashed line is an upper limit for the crystal clear transparency and validity of the calculations.

Down conversion from 1064 nm is possible also with BGSe, covering its entire transmission range in the mid-IR. Radiation at 6.45 µm, e.g. can be generated by oe-e interaction in the *y*-*z* plane or ee-o and oe-o interactions in the *x*-*z* plane. In any case, the best configuration will depend on the values of the nonlinear coefficients. Under Kleinman symmetry, there are four, instead of only two as for BGS, non-zero non-diagonal elements d_{il} for the monoclinic BGSe and the measurement of d_{il} for BGS and BGSe will be the main focus of our future work.

5. Conclusion

In conclusion, we grew the wide bandgap nonlinear crystals BGS and BGSe, and established that these two new compounds possess attractive phase-matching properties for down conversion of 1064 nm radiation into the mid-IR.

References:

1. V. Petrov, F. Noack, I. Tunchev, P. Schunemann, and K. Zawilski, "The nonlinear coefficient d_{36} of $CdSiP_2$", Proc. SPIE **7197**, 71970M (2009).
2. B. Eisenmann, M. Jakowski, and H. Schäfer, „Data on $BaAl_4S_7$ and $BaGa_4S_7$", Rev. Chim. Miner. **20**, 329-337 (1983).
3. X. Lin, G. Zhang, and N. Ye, „Growth and characterization of $BaGa_4S_7$: A new crystal for mid-IR nonlinear optics", Cryst. Growth & Design **9**, 1186-1189 (2009).